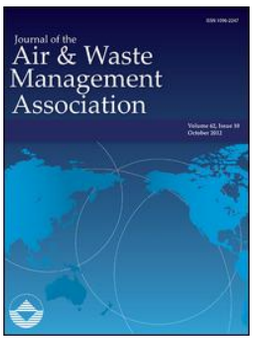

Taylor & Francis
Taylor & Francis Group

Journal of the Air & Waste Management Association

ISSN: 1096-2247 (Print) 2162-2906 (Online) Journal homepage: http://www.tandfonline.com/loi/uawm20

Assessment of Health Effects of Fluctuating Concentrations Using Simplified Pharmacokinetic Algorithms

Bernard E. Saltzman

To cite this article: Bernard E. Saltzman (1996) Assessment of Health Effects of Fluctuating Concentrations Using Simplified Pharmacokinetic Algorithms, Journal of the Air & Waste Management Association, 46:11, 1022-1034, DOI: 10.1080/10473289.1996.10467538

To link to this article: https://doi.org/10.1080/10473289.1996.10467538

TECHNICAL PAPER

ISSN 1047-3289 *J. Air & Waste Manage. Assoc.* **46**: 1022-1034

Assessment of Health Effects of Fluctuating Concentrations Using Simplified Pharmacokinetic Algorithms

Bernard E. Saltzman

Department of Environmental Health, University of Cincinnati, Cincinnati, Ohio

ABSTRACT

The purpose of this study was to develop a simple, practical method to improve the accuracy of assessing health effects by determining the concentration patterns inside the body resulting from fluctuating external pollutant concentrations. Linear pharmacokinetic processes were assumed, and the attenuations of the high- and low-frequency components of the external pattern when entering through the "biological window" were determined. Similar attenuations also were determined for the "time-averaged sampling window." It was shown that when the averaging time was less than 1/4 of the biological half-life, no information of biological significance was lost. Thus, a simple arithmetic step equation was proposed to convert external time-averaged concentrations to "biologically effective concentrations" proportional to internal concentrations. Calculations could readily be made in real time by a monitoring instrument, or even with a pocket calculator. Another simple algorithm was proposed for determining a "biological damage parameter" representative of cumulative damage if the body repair process is slow. Finally, simple algorithms were proposed for calculating body burdens from total absorbed mass rates, a procedure that should be useful for pollutants such as lead that may enter the body through multiple pathways. Results were compared with experimental and hypothetical data to show their utility.

INTRODUCTION

The rising burdens and costs of environmental regulations and the limitations of available financial and human resources have intensified the need to prioritize policy-making decisions. Many legislative proposals now being considered require risk assessment and its cousin, cost-benefit analysis. The main problems in health risk assessment are its complexity and the fact that good data are not available. The very large safety factors commonly used may needlessly raise costs of control to excessive levels. The high costs in time and money of getting the necessary data for the thousands of chemicals of concern make it unlikely that this situation will improve soon. The purpose of this investigation is to develop a simple, practical method for assessing health effects that, by applying scientific principles, makes better use of the data now available.

Current standards commonly are based on averaging pollutant monitoring data for time periods such as 1, 3, 8, or 24 hours, or for longer periods such as one year. However, the health effects of a pollutant relate more accurately to its concentration inside the body, rather than to its concentration on the outside. When external concentration patterns fluctuate, as they commonly do, the internal concentration patterns may differ significantly. Moreover, the internal concentration pattern may depend upon the exposure pattern just prior to the evaluation period, which is ignored by the current standards. In this study, a simplified pharmacokinetic algorithm is proposed that can be readily calculated by a monitoring instrument to continuously convert external concentrations to "biologically effective concentrations" proportional to internal concentrations. The only data required are the biological half-life of the pollutant (a first order approximation) and the air sample averaging time, which best should be less than one quarter of the half-life. Although the biological half-life data are approximations of a very complex biological process, we believe the results should be of a useful degree of accuracy.

IMPLICATIONS

The rising costs of environmental regulations have resulted in proposals to require risk assessment and cost-benefit analysis. Very large safety factors are commonly required for assessing health effects from time-averaged sample data of fluctuating pollutant concentrations. Health effects are more closely related to concentrations inside the body. This theoretical study made reasonable approximations to the complex biological processes, and resulted in simple practical algorithms that can be applied on a real-time basis by a monitoring instrument to determine biologically effective parameters. These should lead to improved standards and help avoid needlessly expensive controls.

APPLICATION TO EXPERIMENTAL CARBON MONOXIDE DATA

The importance of calculating internal concentrations has long been recognized for carbon monoxide. Carbon monoxide combines reversibly with hemoglobin in the blood with 210-250 times the affinity of oxygen, and thus interferes with its oxygen transport. Extensive reviews of the scientific literature describing this action are available in the NIOSH[1] and EPA[2] criteria

documents on carbon monoxide. The Coburn equation[3] is the basis for most of these calculations of carboxyhemoglobin concentrations. Although it is readily applied to constant external concentrations, using it for the infinite variety of possible fluctuating patterns is problematic.

Saltzman[4,5] and Saltzman and Fox[6] suggested a generalized approach based on the fact that any finite fluctuation pattern can be closely approximated as its discrete Fourier transform (i.e., as the sum of a series of sine and cosine waves of differing periods and amplitudes). The sine and cosine components for a given period may be combined into a single sine wave with a specified phase angle and amplitude. If linear kinetic processes for entry of the pollutant into the body are assumed, then the entry of any complex concentration pattern may be determined by adding the entries of each component sine wave and of the mean concentration value.

Therefore, Saltzman and Fox made an experimental study[6] of exposures of rabbits to sine wave concentrations of carbon monoxide with periods of 37 to 280 minutes, and determined the percent carboxyhemoglobin in the blood by analyzing small samples drawn with a catheter implanted in the central aural artery.

Figure 1 presents their experimental data for the run with a sine wave period of 36.8 minutes, and Figure 2 presents their data for a period of 180 minutes. The top section of each figure shows the external concentration pattern, and the points in the middle section give the experimental analyses for the percentage of carboxyhemoglobin in the blood of the exposed rabbit.

On the basis of material balances and of absorption at rates directly proportional to the concentration difference between carbon monoxide in the lungs and its reverse equilibrium pressure in the blood, the fitted curves in the middle sections were plotted from an equation derived by them for exposure to a single sine wave. This equation has only two parameters—the biological half-life of carboxyhemoglobin

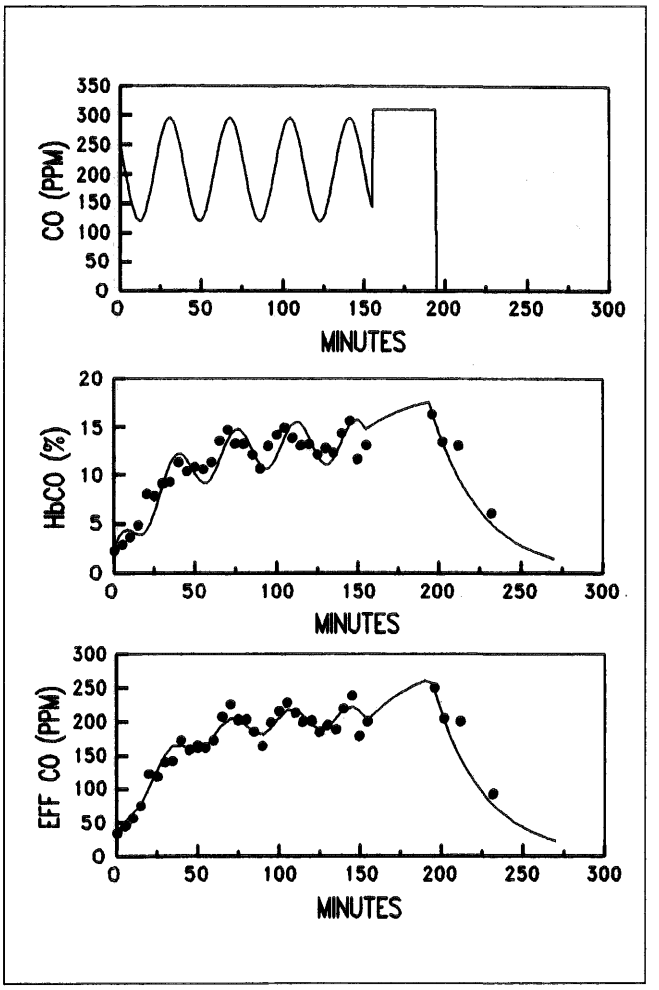

Figure 1. Top section: Sine wave input of CO (mean = 207.5 ppm, amplitude = 87.5 ppm, period = 36.8 min, phase time = -15.3 min) for 155 min, then 287 ppm for 39 min, and then pure air. Middle section: Points are analyses of small samples of blood from an exposed rabbit. Fitted solid curve is Eq.16 with R = 15.33, t_b = 31.86 min. Bottom section: Points are analyses multiplied by R. Fitted solid curve is Eq.1 with t_a = 5 min.

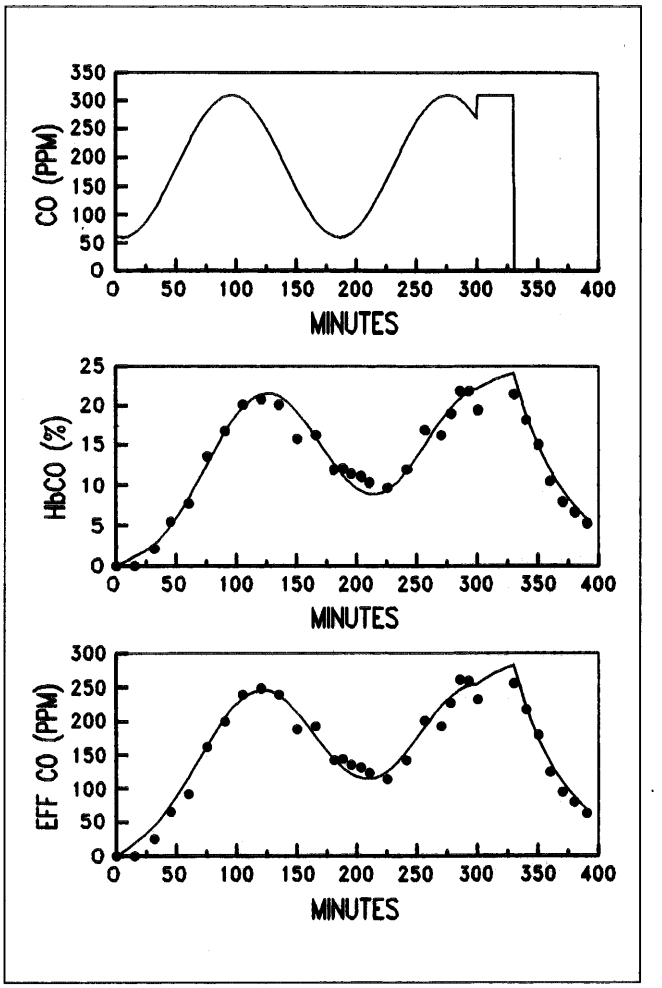

Figure 2. Top section: Sine wave input of CO (mean 185 ppm, amplitude 125 ppm, period 180 min, phase time = 51 min) for 300 min, then 310 ppm for 30 min, and then pure air. Middle section: Points are analyses of small samples of blood from an exposed rabbit. Fitted solid curve is Eq.16 with R = 11.89, t_b = 29.58 min. Bottom section: Points are analyses multiplied by R. Fitted solid curve is Eq.1 with t_a = 5 min.

in the rabbit and R, the *in-vivo* equilibrium ratio of ppm carbon monoxide in the air to the percentage of carboxyhemoglobin (COHb) in its blood. The curves fit the points quite well, within experimental error. The same equation is derived in a simpler generalized way for any pollutant in the appendix of this paper.

The percentage of COHb experimental points have been multiplied by the values of R to give "biologically effective" ppm of carbon monoxide, which are plotted as the points in the bottom sections of Figures 1 and 2. The solid lines in the bottom sections show the results obtained by the proposed simplified algorithm, using air sampling averaging times of five minutes. It is not necessary to know the value of R for this calculation, only the value for the biological half-life.

The simplified algorithm is applied in a stepwise manner to each time-averaged external concentration value, C_i, to convert it to a "biologically effective" value, Y_i, as follows:

$$Y_i = F\,C_i + (1 - F)\,Y_{i-1} \qquad (1)$$

where the biological response fraction, F, is a constant defined by the averaging time, t_a, and the biological half-life, t_b, as:

$$F = [1 - e^{(-0.693 t_a / t_b)}] \qquad (2)$$

The initial value Y_0 may be assumed. Any error in this assumption becomes infinitesimal after three or four biological half-lives.

It can be seen that the results of this simple calculation provide an adequate fit to both fluctuation patterns. The health effects assessed from the original carbon monoxide ppm patterns clearly would be less accurate than those from the calculated "biologically effective" ppm concentrations, regardless of the relatively small errors resulting from assuming simple linear kinetic relationships in a one-compartment model.

THEORETICAL BASIS FOR THE ALGORITHM

In the appendix, a theoretical equation is derived relating internal to external sine wave concentration patterns based on linear kinetic processes in a one-compartment model. The internal response to a constant external concentration is an exponentially rising concentration according to the factor F, ultimately reaching the external value divided by the equilibrium external/internal concentration ratio, R. To any external component sine wave, the internal response is a sine wave of the same frequency, with an amplitude equal to the external amplitude divided by R, but multiplied by a frequency-dependent transmission factor, T_p. The amplitudes of external high frequency (short period) components of a pollutant concentration pattern are attenuated more than those of low frequency (long period) components during transmission through the "biological window" into the body. These frequency-related attenuations are illustrated in Figure 3 by the solid curve. The vertical axis is the variance transmittance factor, defined for this curve as the square of

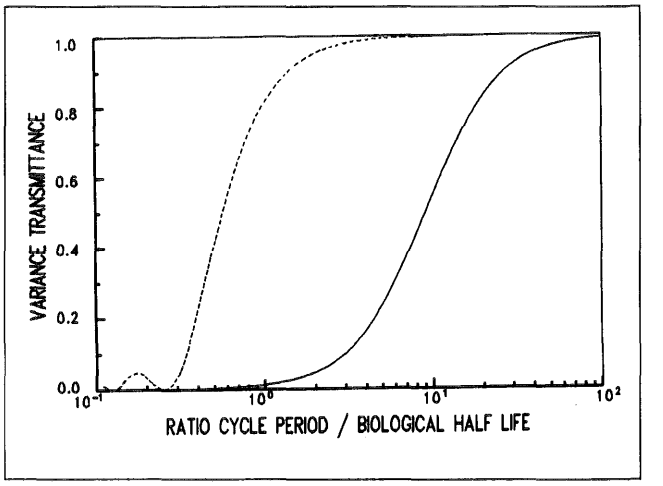

Figure 3. Transmittance of the variances of sine wave components of a fluctuating external concentration pattern through the "biological window" (solid curve) and through the "time-averaged sampling window" (dashed curve), assuming for the latter an averaging time equal to 1/4 of the biological half-life.

T_p. The logarithmic horizontal axis is the ratio of the period of the sine wave to the biological half-life.

The frequency-related attenuations of these external sine wave components during transmission through the "time-averaged sampling window" caused by time-averaging the external concentration pattern also are calculated in the appendix. They depend upon the ratio of the period of the sine wave to the averaging time. The results are given in the dashed curve of Figure 3. The same vertical axis for this dashed curve represents the ratio of the variance per cycle of the external component sine wave, after being time-averaged for many cycles to its original variance per cycle. The horizontal axis assumes that the averaging time is 1/4 of the biological half-life. Other averaging times will move the entire dashed curve horizontally. For example, if the averaging time were equal to 1/8 of the biological half-life, the dashed curve would move to the left by a factor of two.

The figure shows that as long as the averaging time is approximately 1/4 or less of the biological half-life, no appreciable information of biological significance is lost, because the transmittance of the dashed curve is much higher than that of the solid curve in all the regions of significant biological transmittance. This demonstrates that the simple stepwise calculation using constant time-averaged concentration values should give accurate results.

These calculations are based on the simple and readily understood biological half-life parameter. There is great variability in these data and a scarcity of accurate values. A published list[7] of biological half-lives is summarized in Table 1. There is an abundance of monitoring data available, much of which has not been very intensively examined. The U.S. Environmental Protection Agency (EPA) maintains computerized data banks[8] in North Carolina for the Aerometric Information Retrieval System (AIRS) and for Storage and

Table 1. Biological half-lives for some common contaminants.[a]

Substance	Half-Life	Substance	Half-Life
Acetone	3 hr	Iron oxide (fume [Fe_2O_3])	12 hr
Ammonia	< 20 min	Lead[b]	25-40 days
Aniline	2.9 hr	Mercury	5 wks
Benzene	3-5 hr	Methanol	7.0 hr
Benzidine	5.3 hr	Methylene chloride	2.4 hr
Carbon disulfide	0.9 hr	Mineral dust	> 6 mo
Carbon monoxide	1-4 hr	Nitrobenzene	86 hr
Carbon tetrachloride	3 hr	Nitrogen dioxide	1 hr
Chlorine	< 20 min	Phenol	3.4 hr
Chloroform	15-30 min	p-Nitrophenol	1.0 hr
DDT	1-3 yr	Styrene	0.5-8 hr
Dichlorodifluoromethane	9.4 min	Sulfur dioxide	< 20 min
Dimethyl formamide	3.0 hr	Tetrachloroethylene	24-70 hr
Ethyl acetate	2.0 hr	Toluene	12 hr
Ethyl alcohol	1.5-10 hr	1,1,1-Trichloroethane	8.7 hr
Ethyl benzene	5.0 hr	Trichloroethylene	24 hr
Fluorides as F	8 hr	Vinyl chloride	3 hr
Hexane isomers	3.0 hr	Xylene	3.8 hr
Hydrogen sulfide	<20 min		

[a] in humans
[b] in soft tissues; 20 years in bone

Retrieval of U.S. Waterways Parameters (STORET). The various regulatory agencies collect extensive information from all over the country and make it available for analysis.

ILLUSTRATIVE APPLICATIONS OF THE SIMPLIFIED ALGORITHMS

Three illustrations of the use of the proposed simplified methods will be presented. First, the differing internal effects of different concentration patterns, all having the same averages, will be illustrated by applying them to hypothetical data for carbon monoxide. This illustration demonstrates the importance of assessing internal rather than external concentrations. Secondly, a proposed different type of health standard—the biological damage parameter—will be illustrated. And finally, the application of these methods to determining body burdens from lead data will be shown.

Effects of Different Concentration Patterns with the Same Average Concentrations

The differing health effects of various concentration patterns with the same average concentrations may be illustrated by applying the algorithm to some hypothetical carbon monoxide data. For this example, we will assume that eight 1-hr samples are collected successively from three different concentration patterns, CA, CB, and CC, giving values as listed in the first four columns of Table 2. Note that the CA values are all 9 ppm values, the EPA 8-hr standard. The CB values are all in ascending order and average 9 ppm, and the CC values are the same numbers in scrambled order. To illustrate the effects of shorter sampling times, each hourly concentration in the CC pattern was expanded into four widely different 15-minute concentrations having the same average, producing the CD pattern. These concentrations are all illustrated in the top of Figure 4.

We may calculate the biological half-lives of carbon monoxide in humans from the equations given on pages XI-1 and XI-2 in the NIOSH criteria document.[1] They are for people doing sedentary, light, and hard work for 4.2, 1.8, and 1.1 hours, respectively. The human value for R for the ratio of ppm CO to the percentage of carboxyhemoglobin (COHb) in blood is about 6 ppm for levels up to 100 ppm CO. We will assume a half-life of 4.2 hours in this example.

Applying Eq. 2 to a value of $t_a/t_b = 1/4.2$, we get $F = 0.152$, which was entered into Eq. 1. For Case 1, let us assume that previous exposures were to clean air, and that Y_o values were zero in all three patterns. For each of the values of CA entered in succession as C_i in Eq. 1, we calculated the corresponding values of Y_i. This biologically effective concentration pattern is listed as YA in the fifth column of Table 2. The same procedure applied to the CB values yielded the YB pattern, listed in the sixth column, and

Table 2. Carbon monoxide concentration patterns.

	External PPM			Biologically effective PPM					
				Case 1			Case 2		
Hour	CA	CB	CC	YA	YB	YC	YAA	YBB	YCC
0	-	-	-	0	0	0	9	9	9
1	9	2	3	1.37	0.30	0.46	9	7.94	8.09
2	9	3	6	2.53	0.71	1.30	9	7.18	7.77
3	9	5	14	3.51	1.37	3.23	9	6.85	8.72
4	9	6	19	4.35	2.07	5.63	9	6.72	10.28
5	9	10	10	5.06	3.28	6.30	9	7.22	10.24
6	9	13	5	5.66	4.76	6.10	9	8.10	9.44
7	9	14	13	6.16	6.16	7.15	9	9.00	9.98
8	9	19	2	6.60	8.12	6.36	9	10.52	8.77

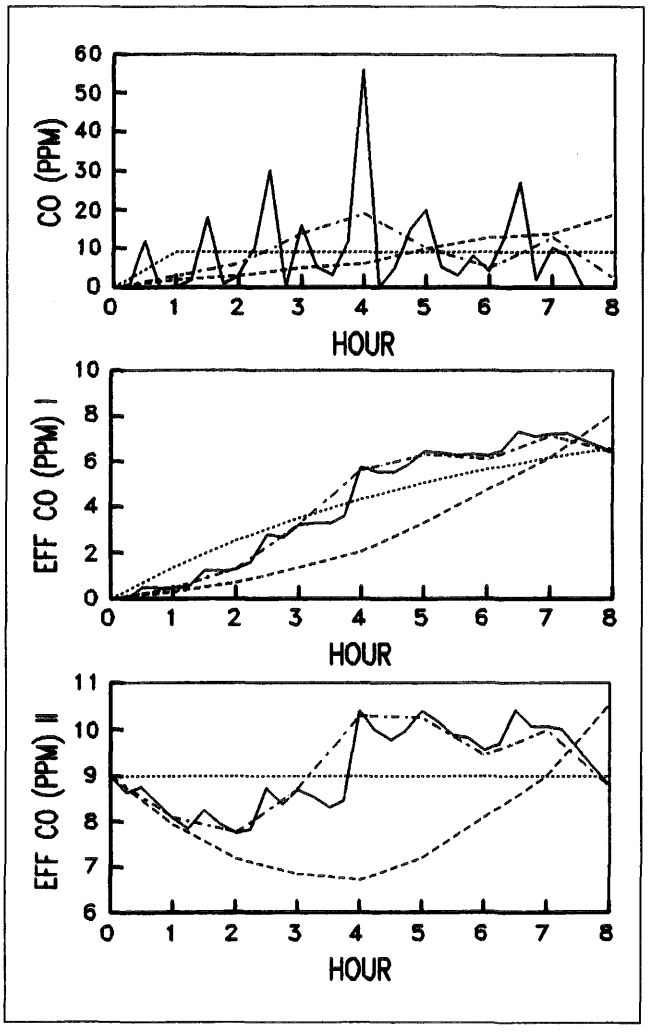

Figure 4. Top section: Ambient carbon monoxide concentration patterns all having an 8-hr time-weighted average of 9 ppm. CA ....., CB ------, CC _._._._, CD _____. Middle section: Corresponding calculated values for the biologically effective ppm for Case 1 (initial ppm = 0). Bottom section: Same for Case 2 (initial ppm = 9 ppm).

applied to CC values, it yielded the YC pattern listed in the seventh column of Table 2. These three patterns are plotted in the middle of Figure 4. The same procedure was applied to the CD pattern, using the value $F = 0.0404$ derived from the different value of $t_a = 1/4$ hr. These calculated values of YD also are plotted in the figure.

For Case 2, let us assume that the previous exposures were to a constant level of 9 ppm for long enough to make Y_o equal to 9 ppm. The calculations were repeated as above, yielding values YAA, YBB, and YCC, listed respectively in the eighth, ninth, and tenth columns of Table 2, and plotted in the bottom of Figure 4 (including pattern YDD).

Comparing the three plots in Figure 4, we see three entirely different pictures. The biologically effective concentrations, which are proportional to the internal concentrations, are not at all like the external concentrations. It is evident that the latter do not give an accurate picture of the possible biological significance of the exposures.

The biologically effective values for pattern YA in the middle of Figure 4 show an exponentially rising curve ending at 6.60 ppm. Those for pattern YB rise more sharply to an ending of 8.12 ppm. The values of Y for pattern YC show a peak of 7.15 ppm at the end of the seventh hour. The YD pattern follows the YC pattern fairly closely. The largest peak deviation is for the 6.5 hr peak of 7.32 ppm, which compares with the YC pattern peak of 7.15 ppm for the seventh hour, a 2% underestimate of the maximum value.

Comparison of the bottom plot of Figure 4 with the middle plot shows that the initial level of biologically effective concentration, Y_o, has a substantial effect on the resulting internal concentration patterns. As expected, the YAA pattern is a straight horizontal line at 9 ppm. The YBB pattern takes a deep dip, and then rises to 10.52 ppm at the end. The YCC pattern peaks at 10.28 ppm at the end of the fourth hour. The YDD pattern follows the YCC pattern closely, peaking at 10.40 ppm at 6.5 hr. Thus, the YCC pattern underestimates the true peak value by 1%, which may be considered a negligible error.

It is evident that although all the patterns have the same 8-hr mean external concentrations, the biologically effective concentration patterns permit more precise evaluations and reduce the needed safety factors. Dividing these effective values by the 6.0 value of R yields the actual values of the percentage of COHb (e.g., 7.32 ppm becomes 1.22% COHb). The natural level of the percentage of COHb produced by metobolic processes from other sources may be added to these values. (Note that linear kinetic relationships permit the addition of various component concentrations.) These levels may be compared to the level of 5% COHb, which is considered undesirable.

The activity level of the individual may change the biological half-life of carbon monoxide. If necessary, allowances may easily be made in these calculations for changing the values of t_b and t_a in some of the time-averaged intervals by using the different appropriate values of F in Eq. 1.

The equations also may be used to calculate short-term limits from the EPA 9 ppm 8-hr average standard, by assuming a standard internal concentration in equilibrium with a long, continued 9-ppm exposure. Thus, the standard for the biologically effective concentration would be also 9 ppm. Inserting this as Y_i in Eq. 1, we may calculate the maximum allowable value C_i by assuming Y_{i-1} is zero. For one hour, this is $9/0.152 = 43.4$ ppm. Similar calculations for workers doing light and hard work using values for t_b of 1.8 hr and 1.1 hr, respectively, yield the corresponding 1-hr maximum allowable external concentrations C_i of 28.1 ppm and 19.31 ppm. These may be compared with the EPA 1-hr maximum allowable value of 35 ppm. If these values are exceeded, the maximum allowable internal concentration will surely be exceeded, even if the initial value before the exposure is as low as zero.

Algorithm for Calculating the "Biological Damage Parameter"

For some pollutants, the internal concentration in the body may not itself be damaging, but it may produce damaged tissue or a toxic product at a rate proportional to its value. Mathematically, this is equivalent to transfer to a second compartment, which may be a critical organ or imaginary in the body. There also may be a process of repairing the damage, with a biological half-life t_d, from which we can calculate a value of F_d using Eq. 2 and the same value as before for t_a. The same equations used above may be applied, using the same time steps for the calculations. In Eq. 1, instead of the time-averaged external concentration C_i, we could substitute the mean of the initial and final internal concentration X for the step. Since the biologically effective concentration is proportional to X and is readily calculated from the data, it is more convenient to use it for this parameter. The author defines the "biological damage parameter," designated as Z, by the following equation:

$$Z_i = F_d\left(\frac{Y_i + Y_{i-1}}{2}\right) + (1 - F_d)Z_{i-1} \qquad (3)$$

For this calculation to be valid, there must be a negligible reverse flow to the first compartment of the original pollutant from reverse equilibrium with the damage product in the second compartment. The reaction must be substantially irreversible. Otherwise Eq. 1 is not valid for the previous calculations of Y_i because the input to the first compartment is not proportional to the external concentration.

The results from Eq. 3 may be illustrated by the following hypothetical application. We assume biological half-lives of 4.2 hr for the pollutant, and 24 hr for repair of the damage by the body. We also assume previous exposure to zero external concentrations, resulting in an initial biologically effective concentration of zero. For the first eight hours of each of five days, we assume the external concentration values shown as CC in the fourth column in Table 2, and for the remainder of each day and for the sixth and seventh day, we assume zero concentration. This pattern is illustrated as the solid line in the top plot of Figure 5. The peak values are 19 ppm during the fourth hour and 13 ppm during the seventh hour of each of the first five days.

Applying the algorithm for biologically effective concentration, using Eq. 1 as before, produces the results illustrated as the solid line in the middle plot of Figure 5. The daily peaks also occurred on the seventh hour, and were 7.15 ppm for the first day and 7.29 ppm for the next four days. It is evident that these concentrations rise and fall more slowly, resulting in broader bases to the peaks. At the end of each day of exposure, the effective concentration still had not fallen to zero. Thus, the second-day peak was higher because the biologically effective concentration began the day higher than the first day. The effect continued for each subsequent day, but became smaller and smaller.

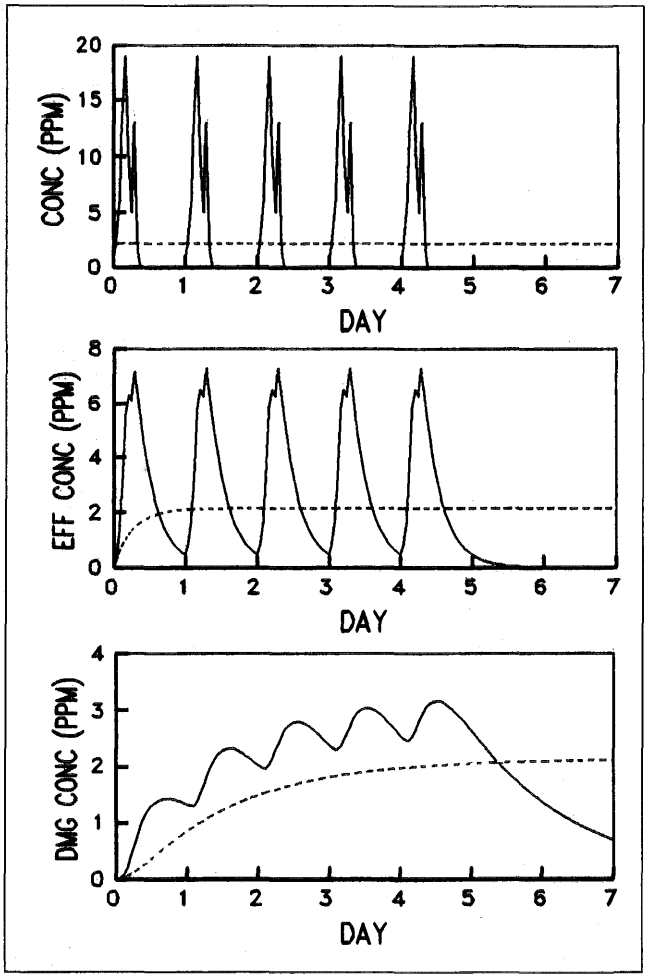

Figure 5. Top section: Varying ambient concentration pattern (solid curve) and constant concentration pattern having the same mean value (dashed curve). Middle section: Corresponding calculated values for the biologically effective concentrations. Bottom section: Corresponding calculated values for the biological damage parameter, assuming a 24-hr half-life for damage repair.

The results for the biological damage parameter obtained by applying Eq. 3 are shown as the solid line in the bottom plot of Figure 5. The concentrations broadened and smoothed into a sine-like curve, and continued to rise until the fifth day. At the end of the seventh day, the level still had not fallen to zero. The peak concentrations in order for the first five days are 1.43 ppm at the end of the 17th hour, 2.32 at the end of the 14th hour, 2.80 at the end of the 13th hour, 3.04 at the end of the 13th hour, and 3.16 at the end of the 12th hour, respectively. If the cycle were to continue for a second week, all the values would start at an initial value of 0.69 ppm, and thus would be higher. It might take several weeks to reach constant peak values on the fifth day.

It is interesting to compare these effects of the exposure pattern to those from a constant average concentration of the same mean. For this illustrative example, the mean concentration = 360/168 = 2.14 ppm. The calculations were made in the same way as above for Figure 5. The data and results are plotted as the dashed lines in Figure 5. The external

concentration was, of course, a straight line at the average value. The biologically effective concentration rose exponentially toward the end, reaching 50% of 2.14 ppm shortly after the 4th hour, and 95% in the 18th hour. The biological damage parameter also rose exponentially toward the end, reaching 50% of 2.14 ppm between the 30th and 31st hour, and 95% in the 110th hour. The maximum values of 2.14 ppm achieved by both of these variables during the week were much lower than the peaks plotted as the solid lines.

Exposure to a fluctuating weekly pattern of pollutants thus could accumulate slowly repaired damage to significantly high levels over a period of days or weeks. If the biological damage repair process is rapid, then the damage pattern more closely resembles the biologically effective concentrations, although the peaks would be somewhat broader. The biological damage parameter thus shows the delayed and accumulative effects of pollutants. It should be useful for some pollutants if appropriate biological half-lives for the damage repair processes are available.

Algorithm for Calculating Body Burdens of Pollutants

Some pollutants may enter the body compartment via multiple pathways, such as from the lungs, the gut, the skin, and also from a very large body sink, such as the bones, if the soft tissues are considered as the body compartment. Thus, it is difficult to evaluate the hazard from the concentrations arriving through a single pathway or through only some of the pathways. For such a situation, it is convenient to use as variables the total mass rates into and out of the body, rather than concentrations, and to use the body compartment burden in terms of the mass of the pollutant.

As was done before for concentration data, we can approximate a fluctuating pattern of the total mass flow rate by a series of time-averaged values for an appropriate averaging period. For such a stepwise calculation, the algorithm derived in the Appendix equivalent to Eq. 1 is:

$$B_i = \left(\frac{F\,t_b}{0.693}\right) M_i + (1 - F) B_{i-1} \qquad (4)$$

where B_i = total body burden of the pollutant after interval i; and M_i = time-averaged total mass flow rate into the body during the interval i. The value of M_i is obtained by adding the mean rates entering through all pathways. The exiting mass rates are not included in this sum. They are allowed for in the B_{i-1} term.

If M is held constant for a very long time, the value of F becomes equal to one, the second term on the right side drops out, and B becomes the equilibrium body burden. Under these conditions, the mass rates both entering and leaving become equal. For a given body burden, we can derive the equilibrium mass rate, m, from Eq. 4:

$$m = (0.693/t_b)B \qquad (5)$$

The applications of these equations are illustrated next by an example with some hypothetical lead data.

A recent publication[9] on lead, cadmium, zinc, and copper in the tissues of 55 human cadavers, on which autopsies were conducted during 1970-1971, presented data for people exposed to the "normal" Cincinnati environment. To get total quantities, metal analyses for each of 29 tissues were multiplied by their estimated fractions of total body weight and by the standard male weight of 70 kg. The mean total lead burden was reported as 88.3 mg in the bones (total weight 10 kg) and as 7.2 mg in the soft tissues (total weight 60 kg). The mean age of the subjects was 50.3 years. The bone lead burden increased with age at 2.27 mg/yr, and the soft tissue lead burden remained constant with age. Reasonable values[7] for the biological half-lives of lead are 30 days in the soft tissues and 20 years in bone.

In this hypothetical illustration we use the above data. A 60-week pattern of weekly-average absorbed lead rates is assumed as follows:

2 mg/day: week 53
1 mg/day: weeks 1-4, 27-30
0.2 mg/day: weeks 13-16, 39-42
0 mg/day: weeks 5-12, 17-26, 31-38, 43-60.

These rates are shown in the top plot of Figure 6. We will apply Eqs. 2, 4, and 5 to calculate the lead burdens in the soft tissues and in bone for 60 weeks.

In Eq. 2, the ratio t_a/t_b for soft tissues is 7/30, yielding F = 0.149; for bone it is 7/7300, and F_b is 0.00066. The values of m from Eq. 5 give the rates at which lead leaves each compartment. The initial rate, m, for soft tissues is 0.166 mg/day, and for bone, mb, is 0.0084 mg/day. The initial net rate entering the bone is 2.27 mg/yr, or 0.0062 mg/day. Thus, the total rate entering the bone is 0.0084 + 0.0062 = 0.0146 mg/day. Dividing this by 0.166, the total rate leaving the soft tissues gives a ratio, r, of 0.088. The kinetic rate constant for lead leaving the soft tissues is composed of the sum of constants for the various component flows. It may be reasonably assumed that over the range of these calculations, the rate going into bone remains in the same ratio to the total rate leaving the soft tissues.

We now apply sixty stepwise calculations for the soft tissues and for the bone respectively, using Eqs. 4 and 5. The double letter variables BB or mb refer to the bone compartment, and an appended 2 indicates a corrected second-round calculation value:

$$B_i = \left(\frac{0.149 \times 30}{0.693}\right) \times M_i + (1 - 0.149) \times B_{i-1} \qquad (6)$$

$$m_i = (0.693/30) \times B_i \qquad (7)$$

$$BB_i = \left(\frac{0.00066 \times 7300}{0.693}\right) \times \left(\frac{m_i + m_{i-1}}{2}\right) \times 0.088 + (1 - .00066) \times BB_{i-1} \qquad (8)$$

Note that for the bone burden in Eq. 8, the mean of the m rates for soft tissue corresponding to the body burdens at the beginning and end of each step is used, and multiplied by r to calculate the rate entering the bone (corresponding to the M_i rate in Eq. 4).

In Eq. 6, if the bone burden is very high, the excretion rate of lead from bone to soft tissue should be added to very low rates of M_i. This correction was found to be small for the present calculations, but it was accomplished by a second set of 60 calculations as follows:

$$mb_i = (0.693/7300) \times BB_i \quad (7a)$$

$$B2_i = \left(\frac{0.149 \times 30}{0.693}\right) \times (M_i + mb_i) + (1 - 0.149) \times B2_{i-1} \quad (6a)$$

In the present example, this correction increased the value of the soft tissue lead burden by an amount exponentially rising to less than 0.4 mg at the end, which was not very significant. In the same way, $m2_i$ was calculated from $B2_i$, used in place of B_i in Eq. 7, and $BB2_i$ was calculated from $m2_i$ and $m2_{i-1}$, used in Eq. 8 in place of m_i and m_{i-1}, respectively.

The final results are shown in Figure 6. The solid lines in the top plot show, in mg/day, the assumed weekly-average absorbed lead rates entering the soft tissue compartment from the environment. Note that this is the sum from all pathways, such as through the gut, skin, and lungs. The net entering rate is this value minus the body excretion rate.

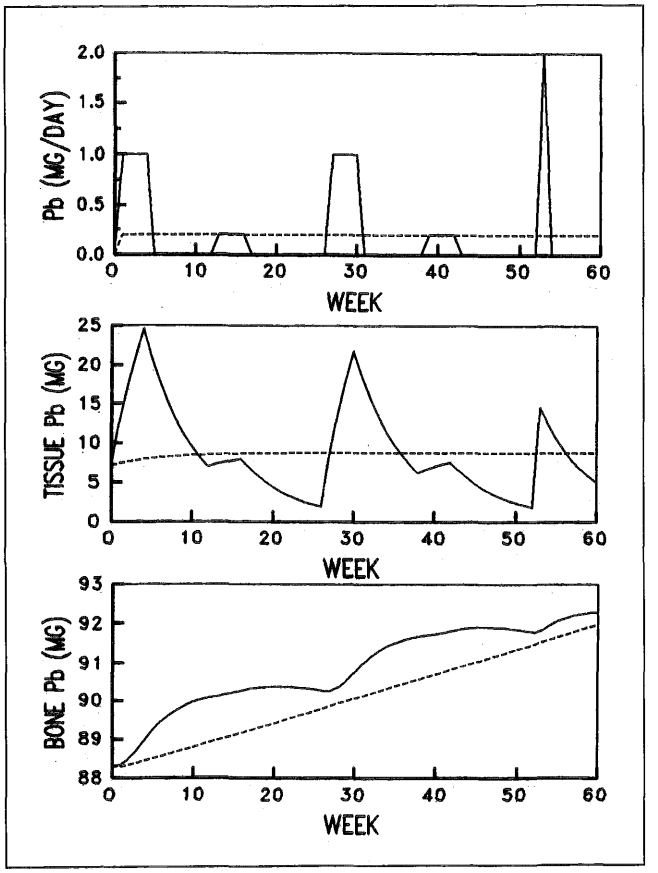

Figure 6. Top section: Varying exposure pattern of absorbed lead rates (solid curve), and constant pattern having the same mean value (dashed curve). Middle section: Corresponding calculated total lead burdens in soft tissue compartment. Bottom section: Corresponding calculated total lead burdens in the bone compartment.

The solid curve in the middle plot shows the soft tissue compartment lead burden in milligrams. It starts at zero week at 7.2, rises exponentially to 24.6 at 4 weeks, falls to 7.0 at 12 weeks, rises to 8.0 at 16 weeks, falls to 1.9 at 26 weeks, rises to 21.8 at 30 weeks, falls to 6.2 at 38 weeks, rises to 7.6 at 42 weeks, falls to 1.8 at 52 weeks, rises to 14.5 at 53 weeks, and falls to 4.9 at 60 weeks.

The solid curve in the bottom plot shows the bone compartment lead burden in milligrams. It starts at 88.3 mg, rises to a peak of 90.4 at 20 weeks, falls to 90.3 at 26 weeks, rises to 91.9 at 46 weeks, falls to 91.8 at 52 weeks, and rises to 92.3 at 60 weeks. Thus, the peaks are long delayed from those in the soft tissues. The exposures at 0.2 mg/day produce only very slight changes in this pattern. It may be seen that the lead is accumulating over the 60 weeks, in spite of the fact that in the 60-week period, there were 43 weeks of zero exposure.

These results for a fluctuating lead absorption rate pattern may be compared with similar calculations made for a constant concentration having the same mean value. This was calculated as (1 wk x 2 mg/day + 8 wk x 1 mg/day + 8 wk x 0.2 mg/day)/60 wk = 0.193 mg/day. Calculations for this constant exposure were made in the same way as above, and results are shown as the dashed lines in Figure 6 for comparisons. The top plot, of course, was a straight line at 0.193 mg/day.

The middle plot for soft tissue burden showed an exponentially rising curve to the end, where it reached 8.75 mg. Because the absorbed lead rate of 0.193 mg/day was only slightly above the initial m (the equilibrium rate of 0.166), the rise from the initial 7.2 mg was slight. An absorbed mass rate lower than 0.166 would show an exponentially falling pattern, and a much higher rate would show a rapidly rising exponential pattern. The values comparable to the peaks for the fluctuating rate exposure were: 7.9 mg at 4 weeks, 8.5 at 12, 8.6 at 16 weeks, and almost constant at 8.7 mg from 26 weeks until the end at 60 weeks.

The pattern for the bone lead burden was a straight line starting at 88.3 mg, and ending at 92.0 mg at 60 weeks. These are comparable to the 91.9 mg maximum at 46 weeks, and to 92.3 mg at 60 weeks for the fluctuating concentration pattern. The fluctuating pattern produces decidedly greater internal effects.

The average absorbed lead rate for the subjects in the cadaver study can readily be calculated from the data. The initial value for m was 0.166 mg/day of lead leaving the soft tissues. Since the soft tissue burden did not increase with age, the value entering was also the same. The 0.008 mg/day entering from the bones was deducted from this amount, leaving 0.158 mg/day of lead as the average rate entering from the environment.

Lead burdens, calculated in milligrams, may be converted to concentration by dividing by the weights of the compartments, 60 kg for the soft tissue, and 10 kg for the bone. The initial soft tissue concentration is thus 7.2/60 = 0.12 ppm. The mean value reported in the cadaver study[9] for blood in the heart and vessels was 0.22 ppm for males and 0.12 ppm for females. The correlation between blood lead and total tissue lead was reported to be a poor 0.37. Although the researchers recognized the possibility that the blood concentrations may have changed in the short intervals between the deaths and the autopsies, they suggested that blood samples, though convenient to collect, may not be too representative of what is in the soft tissues. The study rejected cadavers of individuals known to have been exposed occupationally or otherwise to high lead levels. Dividing the ppm by ten gives the equivalent value in mg/dL.

These types of calculations for pollutants entering the body via multiple pathways should provide a more accurate basis for assessing health effects than using the average external concentrations as a basis.

DISCUSSION

It is important to accurately assess environmental hazards because of their serious health and financial consequences, and because their costs of control are now mounting to the billions of dollars. The illustrations here give evidence that the pollutant concentration patterns inside the body may differ greatly from those outside. The previous history of exposure prior to the evaluation period, as well as the internal pollutant concentration fluctuation patterns during the exposures, may be significant variables that should be taken into account.

Among the difficulties in making an accurate health effects assessment is the complexity of the toxicokinetic processes in the body. Any mathematical model obviously must be an approximation. The proposed simplified methods require three major assumptions: linear kinetics, time-averaged concentrations, and a one-compartment model; in some cases, there is a second compartment with little or no reverse flow to the first compartment.

Linear kinetics have been successfully used to approximate many complex chemical reactions, with recognition that they apply only over a limited range of concentrations. At very high concentrations, deviations may occur because of saturation of body processes (e.g., of hemoglobin in blood by carbon monoxide); however, within the range not greatly exceeding the health standard, it is unlikely that the body processes would be disturbed to such an extent. If a series of consecutive processes occur and the slowest step controls the overall rate, linear kinetics also may be applied.

The assumption has long been made that time-averaged concentrations can adequately represent the natural patterns. Averaging times have been intuitively selected with consideration of analytical and administrative convenience. The dashed curve in Figure 3 shows the theoretical losses of high-frequency components. If the kinetics do not follow the assumptions of linearity and a single compartment, the transmittance of the "biological window" may differ from the solid curve, but it still should follow a sigmoidal shape. A brief pulsation will be attenuated more than a longer pulsation of the same amplitude for two reasons. First, because the quantity of pollutant entering the body is less, the concentration in the receiving mass will rise less. Second, the peak concentration inside the receiving mass is somewhat delayed from the external peak concentration because of the time taken for diffusion. Backwards diffusion, as well as other dissipation processes, will cause more attenuation as the phase difference angle increases with briefer pulses. These processes also occur if a multiple compartment model approximates the relationships. Thus, the plot in Figure 3 remains qualitatively correct. The plot provides a rational basis for selecting averaging times. If data show significant differences between calculated and experimentally observed high frequency components, the averaging time may be reduced.

A linear model with six compartments representing major types of tissues and organs has been used in some toxicokinetic research. This model requires data for flows and kinetic rates for each compartment. Because these data are not readily available and may differ among individuals according to their genetics, activities, and states of health, the final results must be regarded as approximations. The complex equations cannot readily be applied to fluctuating concentrations, making such models impractical for routine applications.

In the case of a pollutant such as lead, the proposed method considers the actual quantities entering through each pathway, as well as the body burden. It seems reasonable to expect that, even with the approximations made, the method should be more useful than some current methods that consider only the concentration in one medium (e.g., air) and apply an arbitrary safety factor to allow for pollutants entering through other pathways.

The proposed simplified methods require a minimum of data, much of which is available. The final working equations are simple arithmetic difference equations that can be handled readily by any computer, or even with a pocket calculator. Monitoring instruments can easily conduct the calculations on a real-time basis. While the results are admittedly inexact, they present a convenient and much more representative picture than the time-weighted average external concentrations. Their application should make possible more accurate standards based on this new data.

CONCLUSIONS

A theoretical examination of the time-averaging method of sampling pollutant concentration patterns has demonstrated that short-term fluctuations of these patterns are attenuated more than the long-term ones; however, the information lost may not be of biological significance, if the transmittance of the "time-averaged sampling window" is sufficiently

better than that of the "biological window." This occurs when the sample averaging period is less than 1/4 of the biological half-life. Thus, sample averaging periods should not be chosen on a convenient basis alone, but should consider the biological effects of the pollutant. For pollutants with a long biological half-life, such as 30 days for lead in soft tissues, a short sample of a few hours or a day will not give significant results, because such a spike will be greatly attenuated.

Practical methods of evaluation based on reasonable approximations have been presented. The biologically effective concentration is readily calculated from the monitoring data, and is the value at *in-vivo* equilibrium with the internal concentration. The biological damage parameter can be representative of the cumulative damage if the body repair process is slow. Finally, for multi-pathway exposures, total absorbed mass rates and body burdens may be calculated, since no single external concentration may account for almost the entire effect. Simple algorithms, which require only linear difference equations, are presented for these calculations. The processing can be done on any personal computer, or even with a pocket calculator. It is hoped that the algorithms' usefulness will be confirmed by more experimental studies, and that they will make possible more accurate standards and health risk assessments for control of environmental hazards.

APPENDIX

The theoretical bases of the algorithms that have been described are derived below. Although the derivations are complex, the actual calculations using the algorithms are simple, as has already been shown. The terminology of the derivations is given in the nomenclature section.

Linear Kinetic Model for Transmission of Fluctuating Concentrations through the "Biological Window"

The various processes through which pollutants enter the body delay and dampen their concentration fluctuations. A convenient model regards this in terms of the transmission of the "biological window," which is a function of the concentration pattern and linear kinetic factors.

Assuming linear kinetics and uniform mixing in the compartment, a material balance taken for the body compartment exposed to the pollutant yields the following equation:

$$W\,dX = (K_1C - K_2X)\,dt \tag{9}$$

The mass of pollutant absorbed on the left side, the weight of the tissue times the differential increase in internal concentration, dX, is equated to the inward mass flow rate of the pollutant, constant K_1 times the driving force C, the external concentration, minus the sum of the pollutant destruction and excretion rates, constant K_2 times X, all times the differential time increment. Note that K_1C is not necessarily the net inward flow rate, since part of the kinetic constant K_2 may represent the reverse equilibrium of X converting back to C and flowing backwards to the environment. This equation rearranges to:

$$\left(\frac{dX}{dt}\right) = \left(\frac{K_1}{W}\right)C - \left(\frac{K_2}{W}\right)X \tag{10}$$

We now define two constants:

$$k = K_2/W \tag{11}$$

$$R = K_2/K_1 \tag{12}$$

Combining Eqs. 10, 11, and 12 gives:

$$\left(\frac{dX}{dt}\right) + kX = \left(\frac{k}{R}\right)C \tag{13}$$

We now must consider the effects of the infinite variety of external concentration fluctuation patterns. These may be closely approximated as the sum of the mean and of a series of component sine waves of differing periods. Because linear kinetics is assumed, the total internal effect may be calculated by adding the effects calculated for each component. The concentration representing the mean for an interval i, C_i, and a series of sine waves of differing periods t_p and amplitudes A_p may be expressed as:

$$C = C_i + A_p \sin[2\pi(t - u_p)/t_p] \tag{14}$$

The terms u_p allow adjustment for the phases of the waves. Inserting this value for concentration into Eq.13 gives the final differential equation:

$$\left(\frac{dX}{dt}\right) + kX = \left(\frac{k}{R}\right)(C_i + A_p\sin[2\pi(t - u_p)/t_p]) \tag{15}$$

This first-order, first-degree differential equation may be solved by multiplying by the integrating factor e^{kt}. The final result integrated over the interval i from time zero to time t is:

$$X_i = F\,C_i/R + D\sin(E) + (1 - F)\,[X_{i-1} - D\sin(G)] \tag{16}$$

where:

$$F = 1 - e^{-kt} \tag{17}$$

$$D = \frac{A_p}{R\sqrt{1 + (2\pi/kt_p)^2}} \tag{18}$$

$$E = [2\pi(t - u_p)/t_p] - \arctan(2\pi/kt_p) \tag{19}$$

$$G = (-2\pi u_p/t_p) - \arctan(2\pi/kt_p) \tag{20}$$

Eq. 16 can be understood best by considering the three terms on the right side separately. First, assume that the initial concentration, X_{i-1}, is zero, and that the exposure is to a constant concentration, and therefore that the A_p values are zero. Then the second and third terms become zero, and the first term describes the exponential rise of the internal concentration X. At infinite time the first factor F becomes

unity. Thus R is the value of the *in-vivo* equilibrium ratio of external concentration C to internal concentration X. This is not the same as the *in-vitro* equilibrium constant, which includes only the part of the constant K_2 for the reverse equilibrium.

If one now assumes external exposure also to sine wave fluctuations of differing periods t_p and amplitudes A_p, the second term represents the corresponding fluctuating components of the internal concentration. The amplitudes of these components are proportional to A_p/R, and to the additional amplitude transmittance factor, T_p, representing the other factor in the denominator of D:

$$T_p = \frac{1}{\sqrt{1 + (2\pi/kt_p)^2}} \tag{21}$$

This transmittance decreases with shorter fluctuation periods t_p.

The internal sine wave lags behind that of the external wave by a part of the E and G terms, arc tan$(2\pi/kt_p)$. The lag approaches 90 deg as t_p becomes smaller. Dividing the lag angle by 2π, which is the angle of a complete period, gives the ratio of the lag time to the period:

$$\left(\frac{t_L}{t_p}\right) = \frac{\text{arc tan}(2\pi/kt_p)}{2\pi} \tag{22}$$

The third term on the right side of Eq. 16 is an adjustment to the first two terms to make the value of internal concentration on the left side at zero initial time t to be equal to X_{i-1}. Note that F is then equal to zero.

If one now assumes an initial value for the internal concentration, and exposure to zero external concentrations, then most of Eq. 16 drops out, leaving only part of the third term of Eq. 16:

$$X_i = (1 - F)\, X_{i-1} = e^{-kt} X_{i-1} \tag{23}$$

This describes the exponential decay of the internal concentration with time. The time at which X_i/X_{i-1} equals 1/2 is defined as the biological half-life, t_b. Solving Eq. 23 for k in terms of t_b yields:

$$k = \ln(2)/t_b = 0.693/t_b \tag{24}$$

It is convenient for use in the algorithms to have expressions in terms of t_b rather than of k. Substituting the right side of Eq. 24 in place of k into Eq. 17, and changing t to t_a for a time-averaged interval yields Eq. 2. Substituting it for k in Eq. 21 and then squaring the result gives the equation plotted as the solid curve in Figure 3.

The biologically effective concentration, Y, is defined by the author as the value that would be in *in-vivo* equilibrium with the internal concentration:

$$Y = R\,X \tag{25}$$

Eq. 1 for a time-averaged interval is derived by multiplying Eq. 16 by R, substituting zero for A_p, and replacing RX terms by Y terms.

Variance Transmittances of the Time-Averaged Sampling Window

Collecting time-averaged samples of a fluctuating concentration also attenuates the observed variance of the pattern. The effect can be mathematically calculated for each component sine wave, which is conveniently stated in terms of time variable θ by the following equation:

$$c = A_p \sin(\theta) \tag{26}$$

We assume that the value of θ at the beginning of the time-averaging period is α. The averaging time t_a is more conveniently expressed as an angle β for this calculation:

$$\beta = 2\pi t_a/t_p \tag{27}$$

The mean value of c that is observed is defined as:

$$c_i = \left(\frac{1}{\beta}\right)\int_{\alpha}^{\alpha+\beta} A_p \sin(\theta)\, d\theta = \left(\frac{A_p}{\beta}\right)[\cos(\alpha) - \cos(\alpha + \beta)] \tag{28}$$

If many repeated time-averaged samples are collected, α will assume all possible values, and the observed variance s^2 is:

$$s^2 = \left(\frac{1}{2\pi}\right)\int_0^{2\pi} c_i^{\,2}\, d\alpha \tag{29}$$

Certain special exceptions to the above equation occur due to resonance effects when t_a/t_p is a rational fraction. In this case, a series of terms for the possible values of α may be summed. The final results have been shown[4] to differ from the general result given below by a factor varying from 0 to 2, depending upon phase relations. These unique values do not alter the conclusions of this calculation.

The value of the right side of Eq. 28 may be expanded and then squared and entered into Eq. 29, after which it may be integrated and simplified.

The true variance of the component sine wave is:

$$\sigma^2 = \left(\frac{1}{2\pi}\right)\int_0^{2\pi} (A_p)^2 \sin^2(\theta)\, d\theta = (A_p)^2/2 \tag{30}$$

The variance transmittance of the time-averaged sampling window, defined as the ratio of the expanded and simplified Eq. 29 divided by Eq. 30, is then:

$$V_p = s^2/\sigma^2 = (2/\beta^2)\,[1 - \cos(\beta)] \tag{31}$$

We now substitute for the value of the angle β its equivalent from Eq. 27 to get the final expression:

$$V_p = \frac{1}{2\pi^2}\left(\frac{t_p}{t_a}\right)^2\left[1 - \cos\left(\frac{2\pi t_a}{t_p}\right)\right] \tag{32}$$

If we assume a value of $t_b/4$ for the value of t_a in the above equation, we can plot the result as the dashed line in Figure 3. For the component fluctuation having the value of t_p/t_b equal to 2, this time-averaged sampling window transmits 95.0%, versus 4.6% for the biological window. The attenuation of shorter-period components caused by time-averaging is of no practical significance, since practically none of them are transmitted by the biological window. Thus, selecting a shorter averaging time would involve collecting more samples without significantly improving the evaluation of biological effects. For longer-period components, the transmission increases above 95.0%, and is adequate for practical purposes.

If we assume a ratio of 1 rather than 1/4 for t_a/t_b, the effect is to move the dashed curve to the right by a factor of 4. Thus, collecting samples averaged for time periods equal to the biological half-life of the pollutant could cause some error in its biological evaluation, if the concentration fluctuation pattern has a significant amount of short-period components.

Equation for Body Burdens of Pollutants

The mathematical relationships are readily derived from the previously listed equations. We may define the entering mass rate in Eq. 9 as K_1C. For our purposes, the total entering mass rate M is the sum of the rates from all j pathways:

$$M = \sum_j (K_1)_j C_j \tag{33}$$

Thus, multiplying a concentration by an appropriate K_1 constant converts it to a mass rate. The entire derivation beginning with the differential equation may be carried out as before, but in terms of a fluctuating mass rate.

The final result may be obtained more simply from Eq. 1. If we multiply all the terms in Eq. 1 by W/R, the left side becomes the body compartment burden, B_i:

$$W\,Y_i/R = W\,X_i = B_i \tag{34}$$

The first term on the right side becomes $F\,C_i\,W/R$. Dividing Eq. 11 by Eq. 12 and rearranging the result shows that $W/R = K_1/k$. Combining this with the value of k from Eq.24 makes the first term become a function of a mean mass rate:

$$F\,C_i W/R = F\,K_1\,C_i/k = F\,M_i/k = \left(\frac{Ft_b}{0.693}\right) M_i \tag{35}$$

The second term on the right of Eq. 1 becomes:

$$(1 - F)\,Y_{i-1}\,W/R = (1 - F)\,W\,X_{i-1} = (1 - F)\,B_{i-1} \tag{36}$$

Reassembling these terms yields Eq. 4.

NOMENCLATURE

- A_p amplitude of sine wave component p
- B_i mass body burden at the end of interval i
- B_{i-1} mass body burden at the beginning of interval i
- $B2$ second round calculated B
- BB mass burden in bones
- C concentration
- C_i mean concentration for interval i
- c component concentration
- c_i mean component concentration for interval i
- D term in Eq.16
- E term in Eq.16
- F biological response fraction, defined by Eqs. 2 or 17
- F_b F for bones
- F_d F for damage repair
- G term in Eq.16
- i subscript index for terms, identifying successive time intervals
- j subscript index for terms, identifying different pathways
- K_1 kinetic constant for flows entering a body compartment
- K_2 kinetic constant for flows exiting a body compartment
- k kinetic constant equivalent to the biological half-life
- M absorbed mass rate
- M_i mean absorbed mass rate for interval i
- m equilibrium mass rate
- mb equilibrium mass rate for bone
- p a subscript identifying a component term
- R *in-vivo* equilibrium ratio of external/internal concentration
- s^2 observed variance
- T_p frequency-related transmittance factor through the "biological window" of sine wave component p
- t time
- t_a sample averaging time
- t_b biological half-life of pollutant in the body
- t_d biological half-life of damage being repaired in the body
- t_L lag time
- t_p period of sine wave component p
- u_p phase time when sine wave component p equals zero and is rising
- V_p variance transmittance of sine wave component p into "time-averaged sampling window"
- W weight of body compartment
- X pollutant (or derivative) concentration inside body compartment

X_{i-1} X at the beginning of interval *i*

X_i X at the end of interval *i*

Y_{i-1} biologically effective pollutant concentration at the beginning of interval *i*

Y_i biologically effective pollutant concentration at the end of interval *i*

Z_{i-1} biological damage parameter at the beginning of interval *i*

Z_i biological damage parameter at the end of interval *i*

α sine wave angle at start of an averaging period

β interval angle equivalent to sine wave averaging period

θ sine wave angle representing the time variable

σ^2 true variance

ACKNOWLEDGMENTS

This work was supported in part by NIOSH Grant 5 T 42 OH 07091.

REFERENCES

1. National Institute for Occupational Safety and Health. *Criteria for a Recommended Standard - Occupational Exposure to Carbon Monoxide*; Pub. No. (HSM) 73-11000, U.S. Department of Health, Education, and Welfare: Washington, D.C., 1972.
2. National Air Pollution Control Administration. *Air Quality Criteria for Carbon Monoxide*; NAPCA Pub. No. AP-62, U.S. Department of Health, Education and Welfare: Washington, DC, 1970.
3. Coburn, R.F.; Forester, R.E.; Kane, P.B. *J. Clin. Invest.* **1965**, *21*, 1899.
4. Saltzman, B.E. *J. Air Pollut. Control Assoc.* **1970**, *20*, 660-665.
5. Saltzman, B.E. *U.S. Environmental Protection Agency*, Res. Dev., (Rep.) EPA 1974, EPA-650/4-74-038, pp. 11-1 to 11-13.
6. Saltzman, B.E.; Fox, S.H. *Env. Sci. Tech.* **1986**, *20*, 916-923.
7. Saltzman, B.E. *Am. Ind. Hyg. Assoc. J.* **1988**, *49*, 213-225.
8. Environmental Protection Agency. Access EPA, Pub. No. EPA/220-13-92-014; Environmental Protection Agency, Washington, D.C., 1992.
9. Saltzman, B.E.; Gross, S.B.; Yeager, D.W.; Meiners, B.G.; Gartside, P.S. *Environ. Res.* **1990**, *52*, 126-145.

About the Author

Bernard E. Saltzman is an emeritus professor of environmental health in the College of Medicine, Department of Environmental Health, University of Cincinnati, Cincinnati, OH 45267-0056 (or send e-mail to saltzmbe@ucbeh.san.uc.edu). Previously, he retired from the U.S. Public Health Service after working in its early air pollution and industrial hygiene programs.